Enhanced Paraxylene Selectivity in a Fixed-Bed Reactor

Simulations of enhanced paraxylene selectivity in a fixed-bed reactor are presented in this paper. The primary reaction of alkylation of toluene with methanol and the secondary isomerization of the xylene products occurring inside zeolite catalysts ZSM-5 are considered. The selectivity of paraxylene is enhanced due to the great difference between the effective diffusivities of xylene isomers. Such enhancement is found to decrease with toluene conversion along the reactor. Behaviors of intracrystal concentration profiles of three xylene isomers and toluene are also investigated.

D. D. DO

Department of Chemical Engineering
University of Queensland
St. Lucia, Qld. 4067, Australia

SCOPE

Paraxylene is a valuable product in chemical industries because of large demand for oxidation to terephthalic acid, a major component in polyester fibers, and demand in the synthesis to vitamins and pharmaceuticals. One of the main sources of paraxylene production is the alkylation of toluene with alcohol. This reaction of alkylation produces a primary distribution of xylene isomers at the catalytic site (microscopic level). A typical primary distribution of xylene isomers from a Friedel-Crafts reaction of (*o*: 60%, *m*: 14%, *p*: 26%) has been reported by Allen and Yats (1961). This primary distribution is subsequently changed by the coupling of the physical transport process (pore diffusion) and the isomerization of xylene isomers. This results in the secondary distribution of these isomers at the surface of the catalyst pellet or in the bulk solution. The aim of this paper is to determine how these xylene isomers are distributed in the bulk solution (i.e., secondary distribution) as a function of crystal size, speed of chemical reaction, ratio of reaction rate constants of alkylation to isomerization, ratio of diffusivities, and the degree of conversion of the primary reaction of alkylation of toluene with methanol.

CONCLUSIONS AND SIGNIFICANCE

Enhanced paraxylene selectivity in a fixed-bed reactor was theoretically studied using a method of finite integral transform. The primary distribution of xylene isomers from the reaction of alkylation of toluene with methanol has been shown to influence substantially the secondary distribution of these isomers in bulk solution, especially when the chemical reaction is slow. However, when the chemical reaction is fast (Thiele modulus, ϕ, is greater than about 100) this primary distribution of xylene isomers at the catalytic site has very little influence on the secondary distribution because in this case the macroscopic production of xylene isomers is controlled by the diffusion of these species within the pores. The paraxylene selectivity in the reactor is greatly enhanced for large values of ϕ, that is, for large crystal sizes and high temperatures. The same results are expected to be true for toluene disproportionation reactions, because for large values of ϕ, the paraxylene selectivity in the reactor (i.e., the secondary distribution) is independent of the primary reaction and its distribution of xylene isomers.

INTRODUCTION

Toluene is one of the major products produced in the catalytic reformers of petroleum refineries. Its presence in the reformate increases the octane number of the gasoline. Beside being used as a component in the gasoline, toluene is alkylated with methanol to produce xylenes. Among these xylene isomers, paraxylene is a valuable product because of its high demand for oxidation to terephthalic acid, a major component in polyester fibers. However, the xylene isomers isomerize simultaneously with the alkylation of toluene to reach equilibrium proportion of 22%, 54%, and 24% of ortho-, meta-, and para-xylenes, respectively (Allen and Yats, 1961). Such a mixture of xylenes requires repeated separation and isomerization processes to obtain a certain degree of purity of para-xylene.

Xylene isomerization can be carried out either over amorphous silica alumina (Cortes and Corma, 1978, Chutoransky and Dwyer, 1973; Silvestri and Prater, 1964) or over various types of zeolite (Röbschläger and Christoffel, 1980; Collins et al., 1982). Usually, an equilibrium of 24% of *p*-xylene is observed for most untreated zeolites. A comparison between acid zeolite catalyst and amorphous silica-alumina catalyst was made by Collins et al. (1982), and they found that over LaY zeolite *o*-xylene isomerizes rapidly, while *m*- and *p*-xylenes isomerize at about the same rate, and the amorphous silica alumina catalyst has a lower activity than the zeolite catalyst. The relative rate constants were calculated using Wei's method (1962a).

However, in 1970, Yashima and his coworkers (1970a, b, 1972) reported that about 50% *p*-xylene selectivity was obtained over a variety of cation-exchanged zeolite Y catalyst. Such experimental findings have prompted many investigations into development of

paraselective zeolite catalyst to increase paraxylene in the final product. They indicated that in the alkylation of toluene with methanol, substitution of the methyl group of toluene is para/ortho-orientation and the primary reaction products are supposed to be para and ortho isomers. This indicates reaction mechanisms involving an electrophilic attack on the aromatic ring by carbonium ion intermediates (Venuto et al., 1966). It is important to point out here that the primary xylene isomers' distribution is affected only by the kinetics of the primary reaction of alkylation of toluene. For example, a typical primary distribution of xylene isomers from a Friedel-Crafts reaction is (o, m, p) = (60, 14, 26). The secondary distribution that they observed (50% para selectivity) is in fact affected by the interaction of the xylene isomerization reactions and the intracrystallite diffusion process.

Chen et al. (1979) have also observed better selectivity of paraxylene (46%) for zeolite catalysts having large crystal sizes. Up to 97% paraselectivity was observed in their work with zeolite ZSM-5 modified with phosphorus. This finding will be justified in this analysis. The para-xylene selectivity enhanced by certain zeolite catalysts was explained by Kaeding et al. (1981) that the steric restriction of o- and m-xylenes has helped to increase the outflux of p-xylene. Their diffusion measurements indicate that the diffusivity of p-xylene is 1000 times faster than that of o- and m-xylenes. Their explanation was in line with the pioneering work by Weisz and Frilette (1960) on shape selective catalysts in which the steric restriction produces the secondary distribution of products, which is entirely different from the primary distribution at the catalytic sites.

To provide such steric restriction of o- and m-xylenes, Kaeding et al. (1981) and Young et al. (1982) impregnated the zeolite catalysts with phosphorous or boron compound. The results of such studies have indicated that nearly 100% of paraxylene can be achieved. They found that the p-xylene selectivity is greatly enhanced with an increase in crystal size and temperature. This interesting experimental finding will be qualitatively justified in this paper.

This paraxylene selectivity enhancement was also observed when the zeolite catalyst is subject to coking deposition (i.e., steric restriction is increased) and when the catalyst surface is coated with heat-stable polymers (Kaeding et al., 1981).

Young et al. (1982) have found that at *low* temperatures many modified ZSM-5 type catalysts produced ortho-rich xylene product mixtures. The xylene isomer compositions appear to approach the ratio (o, m, p = 60, 14, 26), shown to be the initial xylene isomer composition in low temperature Friedel-Crafts–catalyzed methylation of toluene. These compositions are also similar to those produced by silica alumina catalyst. This confirms the ortho/para orientation in the alkylation of toluene with methanol.

The reaction network of xylene isomerization has also been studied by many workers. The sequence network of ortho $\rightleftharpoons$ meta $\rightleftharpoons$ para was used by Hanson and Engel (1967), Chutoransky and Dwyer (1973), and Cortes and Corma (1978). The triangular network was used by Silvestri and Prater (1964) and Röbschläger and Christoffel (1980). The reactions for ring opening, cracking, and hydrogenation occur to a limited extent and were taken into account in the work of Röbschläger and Christoffel (1980). The choice of the sequence network will be used in our theoretical study because in the experiments of Cortes and Corma (1978) using deuterium-labeled paraxylene, they confirmed that the mechanism follows intramolecular 1,2 shifts of the methyl group around the aromatic ring.

In this work, we will study the selectivity of paraxylene vs. conversion. The alkylation of toluene with methanol and the isomerization of pure o-xylene will be investigated in the integral fixed-bed reactor. We will make further calculations based on the theory of Wei (1982). The relative effective diffusivities and the relative rate constants for xylene isomerization were taken from Wei (1982). The method employing a finite integral transform is used in this paper to obtain solutions for concentrations in the reactor, the intracrystal concentrations at any location along the reactor, and the paraxylene selectivity versus the toluene conversion.

THEORY

Consider an isothermal fixed-bed reactor continuously fed with toluene and methanol. This mixture of toluene and methanol diffuses into zeolite catalysts packed inside the reactor. The reaction of toluene and methanol at the catalytic sites yields a mixture of o-, m-, and p-xylene and water. The primary distribution of xylenes are f_o, f_m, and f_p, respectively ($\Sigma_{j=o,m,p} f_j = 1$). Here, we assume that methanol is in excess and the diffusion of methanol inside zeolite catalysts is relatively fast so that the quasireaction rate constant for the reaction of toluene may be considered constant throughout the catalyst. The xylenes produced from the toluene reaction isomerize inside the catalyst while they are diffusing out of it (see Figure 2).

One important point to note here is that catalyst pellets are usually employed in a fixed-bed reactor. These are made by compressing the zeolite crystals together with or without binder, and then they are crushed in the proper size range. For example, Yashima et al. (1970a) pelleted the zeolite without binder and then crushed them to 8–14 mesh. Thus the catalyst pellet will have bidisperse pore structure. The macropores are the regions between the crystal (intercrystalline void) and the micropores are the regions inside the crystal (intracrystalline void). Since the diffusion in the micropore (intracrystalline diffusion) is severely restricted, the overall reaction rate of a catalyst pellet will be controlled by the micropore diffusion and reaction. This simply means that there will be no concentration gradient inside the macropores. Therefore, the mass balance equations of a catalyst pellet will involve only diffusion and reaction inside embedded crystals.

Let C_1, C_2, C_3, and C_4 be concentrations of toluene, o-xylene, m-xylene, and p-xylene inside the catalyst pellet; C_{bj} are their counterpart concentrations in the reactor. The mass balance equations inside a porous crystal at any arbitrary location along the reactor are

$$\mathcal{D}_T \nabla^2 C_1 - k_a C_1 = 0 \tag{1a}$$

$$\mathcal{D}_o \nabla^2 C_2 + f_o k_a C_1 - 2k_I C_2 + k_I C_3 = 0 \tag{1b}$$

$$\mathcal{D}_o \nabla^2 C_3 + f_m k_a C_1 + 2k_I C_2 - 2k_I C_3 + 2k_I C_4 = 0 \tag{1c}$$

$$1{,}000\, \mathcal{D}_o \nabla^2 C_4 + f_p k_a C_1 + k_I C_3 - 2k_I C_4 = 0 \tag{1d}$$

where $\mathcal{D}_T$ is the effective diffusivity of toluene, $\mathcal{D}_o$ is the effective diffusivity of o- and m-xylene, 1000 $\mathcal{D}_o$ is the effective diffusivity of p-xylene, k_a is the rate constant for alkylation of toluene, k_I is the rate constant for isomerization, and

$$\nabla^2 = \frac{1}{r^2}\frac{\partial}{\partial r}\left(r^2 \frac{\partial}{\partial r}\right) \tag{2}$$

The relative magnitude of effective diffusivities and rate constants for xylene mixture are taken from Wei (1982). The effective diffusivity of p-xylene is 1000 times greater than those of o- and m-xylenes.

The boundary conditions of Eqs. 1 are

$$r = 0; \qquad \partial C_j / \partial r = 0 \tag{3a}$$

$$r = R; \qquad C_j = C_{bj} \tag{3b}$$

where R is the radius of the crystal. Since we have assumed that the macropore transport is negligible compared to the crystallite transport, the effect of the pellet size will not be seen in our model solutions. Here, we have ignored the external mass transfer resistance at the solid-fluid interface, which is usually the case in most industrial reactors.

The mass balance equations for the species j inside the reactor is

$$\bar{u}\frac{dC_{bj}}{dz} + \frac{3}{R}(1-\epsilon_b)\,\mathcal{D}_j \left.\frac{\partial C_j}{\partial r}\right|_R = 0 \tag{4}$$

where $\bar{u}$ is the superficial velocity, ϵ_b is the bed voidage, and z is the axial coordinate. The initial condition of Eq. 4 is

$$z = 0; \qquad C_{bj} = C_{bj_o} \tag{5}$$

By introducing the following nondimensional variables and parameters

$$u_i = C_j/C_{b1_o}, \quad u_{bj} = C_{bj}/C_{b1_o} \tag{6a}$$

$$u_{bj_o} = C_{bj_o}/C_{b1_o}, \quad x = r/R, \quad t = z/L \tag{6b}$$

$$\phi^2 = R^2 k_I/\mathcal{D}_o, \quad \gamma = \frac{3}{R^2}(1-\epsilon_b)\frac{\mathcal{D}_o L}{\bar{u}} \tag{6c}$$

$$\sigma = \mathcal{D}_T/\mathcal{D}_o, \quad \alpha = k_a/k_I \tag{6d}$$

Equations 1 to 5 become

$$\nabla^{*2}u_1 - \left(\frac{\alpha}{\sigma}\right)\phi^2 u_1 = 0, \tag{7a}$$

$$\nabla^{*2}u_2 + f_o\alpha\phi^2 u_1 - \phi^2(2u_2 - u_3) = 0 \tag{7b}$$

$$\nabla^{*2}u_3 + f_m\alpha\phi^2 u_1 + \phi^2(2u_2 - 2u_3 + 2u_4) = 0 \tag{7c}$$

$$1{,}000\,\nabla^{*2}u_4 + f_p\alpha\phi^2 u_1 + \phi^2(u_3 - 2u_4) = 0 \tag{7d}$$

$$\frac{du_{b1}}{dt} + \sigma\gamma\left.\frac{\partial u_1}{\partial x}\right|_1 = 0 \tag{8a}$$

$$\frac{du_{b2}}{dt} + \gamma\left.\frac{\partial u_2}{\partial x}\right|_1 = 0 \tag{8b}$$

$$\frac{du_{b3}}{dt} + \gamma\left.\frac{\partial u_3}{\partial x}\right|_1 = 0 \tag{8c}$$

$$\frac{du_{b4}}{dt} + 1{,}000\,\gamma\left.\frac{\partial u_4}{\partial x}\right|_1 = 0 \tag{8d}$$

subject to

$$x = 0; \quad \partial u_j/\partial x = 0 \tag{9a}$$

$$x = 1; \quad u_j = u_{bj} \tag{9b}$$

$$t = 0; \quad u_{bj} = u_{bj_0} \tag{10}$$

for $j = 1, 2, 3$, and 4, where

$$\nabla^{*2} = \frac{1}{x^2}\frac{\partial}{\partial x}\left(x^2\frac{\partial}{\partial x}\right) \tag{11}$$

The technique that we are going to use to solve the above nondimensional governing equations is the finite integral transform

$$A = \begin{bmatrix} -\left(\xi_n^2 + \dfrac{\alpha}{\sigma}\phi_2\right) & 0 & 0 & 0 \\ f_o\alpha\phi^2 & -(\xi_n^2 + 2\phi^2) & \phi^2 & 0 \\ f_m\alpha\phi^2 & 2\phi^2 & -(\xi_n^2 + 2\phi^2) & 2\phi^2 \\ f_p\alpha\phi^2 & 0 & \phi^2 & -(1{,}000\xi_n^2 + 2\phi^2) \end{bmatrix}, \tag{22}$$

technique applied to remove the spatial coordinate x. The resulting equations are coupled ordinary differential equations in transform space. These equations are, of course, easier to solve than the original coupled partial differential equations. But before applying the transform technique, we homogenize the boundary conditions by introducing the following transformation:

$$v_j = u_{bj} - u_j \; (j = 1, 2, 3, 4) \tag{12}$$

With respect to the new dependent variables, Eqs. 7, 8, and 9 become

$$\nabla^{*2}v_1 - \left(\frac{\alpha}{\sigma}\right)\phi^2 v_1 = -\left(\frac{\alpha}{\sigma}\right)\phi^2 u_{b1} \tag{13a}$$

$$\nabla^{*2}v_2 + f_o\alpha\phi^2 v_1 - \phi^2(2v_2 - v_3) = f_o\alpha\phi^2 u_{b1} - \phi^2(2u_{b2} - u_{b3}) \tag{13b}$$

$$\nabla^{*2}v_3 + f_m\alpha\phi^2 v_1 + \phi^2(2v_2 - 2v_3 + 2v_4) = f_m\alpha\phi^2 u_{b1} + \phi^2(2u_{b2} - 2u_{b3} + 2u_{b4}) \tag{13c}$$

$$1{,}000\,\nabla^{*2}v_4 + f_p\alpha\phi^2 v_1 + \phi^2(v_3 - 2v_4) = f_p\alpha\phi^2 u_{b1} + \phi^2(u_{b3} - 2u_{b4}) \tag{13d}$$

$$\frac{du_{b1}}{dt} = \sigma\gamma\left.\frac{\partial v_1}{\partial x}\right|_1 \tag{14a}$$

$$\frac{du_{b2}}{dt} = \gamma\left.\frac{\partial v_2}{\partial x}\right|_1 \tag{14b}$$

$$\frac{du_{b3}}{dt} = \gamma\left.\frac{\partial v_3}{\partial x}\right|_1 \tag{14c}$$

$$\frac{du_{b4}}{dt} = 1{,}000\,\gamma\left.\frac{\partial v_4}{\partial x}\right|_1 \tag{14d}$$

$$x = 0; \quad \partial v_j/\partial x = 0 \tag{15a}$$

$$x = 1; \quad v_j = 0 \tag{15b}$$

for $j = 1, 2, 3$ and 4.

We define the following integral transform

$$\langle v_j, K_n\rangle = \int_0^1 x^2 v_j K_n(x)dx \tag{16}$$

where $K_n(x)$ is called the kernel of the transform and is given by

$$K_n = \sin(\xi_n x)/x \tag{17}$$

where ξ_n is its corresponding eigenvalue and is

$$\xi_n = n\pi; \quad n = 1, 2, \ldots, \infty \tag{18}$$

According to Sneddon (1972), the choice of the weighting function x^2, of kernel $K_n(x)$ is unique for a given linear differential operator ∇^{*2} and boundary conditions.

Applying the transform 16 to Eqs. 13, we obtain

$$A\Omega = \phi^2\langle 1, K_n\rangle K\, U_b \tag{18}$$

where

$$\Omega = \begin{bmatrix} \langle v_1, K_n\rangle \\ \langle v_2, K_n\rangle \\ \langle v_3, K_n\rangle \\ \langle v_4, K_n\rangle \end{bmatrix} \tag{20}$$

$$U_b = [u_{b1}, u_{b2}, u_{b3}, u_{b4}]^T \tag{21}$$

$$K = \begin{bmatrix} -\dfrac{\alpha}{\sigma} & 0 & 0 & 0 \\ f_o\alpha & -2 & 1 & 0 \\ f_m\alpha & 2 & -2 & 2 \\ f_p\alpha & 0 & 1 & -2 \end{bmatrix}, \tag{23}$$

and $\langle 1, K_n\rangle$ is the transform of unity and is

$$\langle 1, K_n\rangle = -\frac{\cos\xi_n}{\xi_n} \tag{24}$$

Solution to Eq. 19 is straightforward:

$$\Omega = \phi^2\langle 1, K_n\rangle A^{-1}K\, U_b \tag{25}$$

where the inverse A^{-1} is

$$A^{-1} = \{\beta_{ij}\} \tag{26a}$$

$$\beta_{11} = -1/a \tag{26b}$$

$$\beta_{12} = \beta_{13} = \beta_{14} = 0 \tag{26c}$$

$$\beta_{21} = -\frac{f_o\alpha\phi^2}{ab} - \frac{f_m\alpha\phi^2}{2abd} - \frac{f_o\alpha\phi^4}{ab^2d} - \frac{f_p\alpha\phi^2}{abde} - \frac{f_m\alpha\phi^2}{2abd^2e} - \frac{f_o\alpha\phi^4}{ab^2d^2e} \quad (26d)$$

$$\beta_{22} = -\frac{1}{b} - \frac{\phi^2}{b^2d^2e} - \frac{\phi^2}{b^2d} \quad (26e)$$

$$\beta_{23} = -\frac{1}{2bd} - \frac{1}{2bd^2e} \quad (26f)$$

$$\beta_{24} = -\frac{1}{bde} \quad (26g)$$

$$\beta_{31} = -\frac{f_m\alpha}{2ad} - \frac{f_o\alpha\phi^2}{abd} - \frac{f_p\alpha}{ade} - \frac{f_m\alpha}{2ad^2e} - \frac{f_o\alpha\phi^2}{abd^2e} \quad (26h)$$

$$\beta_{32} = -\frac{1}{bd^2e} - \frac{1}{bd} \quad (26i)$$

$$\beta_{33} = -\frac{1}{2d\phi^2} - \frac{1}{2d^2e\phi^2} \quad (26j)$$

$$\beta_{34} = -\frac{1}{de\phi^2} \quad (26k)$$

$$\beta_{41} = -\frac{f_p\alpha}{ae} - \frac{f_m\alpha}{2ade} - \frac{f_o\alpha\phi^2}{abde} \quad (26l)$$

$$\beta_{42} = -\frac{1}{bde} \quad (26m)$$

$$\beta_{43} = -\frac{1}{2de\phi^2} \quad (26n)$$

$$\beta_{44} = -\frac{1}{e\phi^2} \quad (26o)$$

where

$$a = \left(\xi_n^2 + \frac{\alpha}{\sigma}\phi^2\right) \quad (27a)$$

$$b = (\xi_n^2 + 2\phi^2) \quad (27b)$$

$$c = (1{,}000\xi_n^2 + 2\phi^2) \quad (27c)$$

$$d = \frac{b}{2\phi^2} - \frac{\phi^2}{b} \quad (27d)$$

$$e = \frac{c}{\phi^2} - \frac{1}{d} \quad (27e)$$

Having obtained the solution for Ω, the inverse may be found as an infinite series in terms of the eigenfunction $K_n(x)$:

$$V = \phi^2 \sum_{n=1}^{\infty} \frac{\langle 1, K_n\rangle K_n(x)}{\langle K_n, K_n\rangle} A^{-1}KU_b \quad (28)$$

where

$$V = [v_1, v_2, v_3, v_4]^T \quad (29a)$$

and

$$\langle K_n, K_n\rangle = 1/2 \quad (29b)$$

Thus we have obtained the intracrystal concentration U(or V) in terms of the reactor concentration U_b. Rewriting the mass balance equations in the reactor (Eqs. 14) in vector form, we obtain:

$$\frac{dU_b}{dt} = \gamma D \left.\frac{\partial V}{\partial x}\right|_1 \quad (30)$$

where

$$D = \begin{bmatrix} \sigma & 0 & 0 & 0 \\ 0 & 1 & 0 & 0 \\ 0 & 0 & 1 & 0 \\ 0 & 0 & 0 & 1{,}000 \end{bmatrix} \quad (31)$$

Substituting Eq. 28 into Eq. 30, we have

$$\frac{dU_b}{dt} = -\gamma\phi^2 \sum_{n=1}^{\infty} \frac{\xi_n^2\langle 1, K_n\rangle^2}{\langle K_n, K_n\rangle} D A^{-1}KU_b \quad (32)$$

in which we have used the relationship

$$K_n'(1) = -\xi_n^2\langle 1, K_n\rangle \quad (33)$$

From our definition of kernel K_n (Eq. 17), it is easy to show that

$$\frac{\xi_n^2\langle 1, K_n\rangle^2}{\langle K_n, K_n\rangle} = 2 \quad (34)$$

Therefore, Eq. 32 becomes

$$\frac{dU_b}{dt} = -\gamma\phi^2 C U_b \quad (35)$$

where

$$C = 2\sum_{n=1}^{\infty} D A^{-1}K \quad (36)$$

The initial condition of Eq. 35 is

$$t = 0; \qquad U_b = U_{bo} = [u_{b1_o}, u_{b2_o}, u_{b3_o}, u_{b4_o}]^T$$

Solution to Eq. 35, subject to the initial condition 37, is

$$U_b = \exp(-\gamma\phi^2 t\ C)U_{bo} \quad (37)$$

At any location along the reactor, the toluene conversion and the p-xylene selectivity are

$$X = 1 - u_{b1} \quad (38)$$

and

$$S = \frac{u_{b4}}{u_{b2} + u_{b3} + u_{b4}} \quad (39)$$

respectively.

Knowing the bulk concentration U_b, the intracrystal concentration can be calculated from

$$U = [I - \phi^2 \sum_{n=1}^{\infty} \frac{\langle 1, K_n\rangle K_n(x)}{\langle K_n, K_n\rangle} A^{-1}K]U_b \quad (40)$$

where I is the identity matrix.

DISCUSSION

The solutions for the reactor concentrations (Eq. 37), the intracrystal concentration (Eq. 40), the toluene conversion (Eq. 38), and the selectivity of paraxylene with respect to xylene isomers (Eq. 39) have been obtained analytically in the form of infinite series. It is not difficult to show from Eq. 26 that all the elements of the matrix A^{-1} are of order of at most $1/n^2$, when n is large. Therefore, the absolute convergence of the matrix C (Eq. 36) is ensured.

Before discussing the simulation results, it is pointed out that we have assumed that the effective diffusivity of paraxylene is 1,000 times greater than those of other xylenes, and the relative rate constants for isomerization are taken from Wei (1982). However,

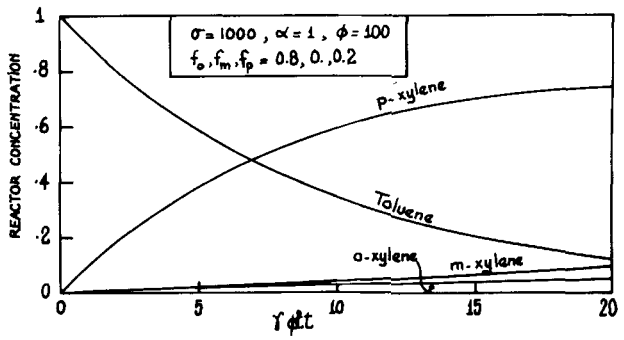

Figure 1. Plots of reactor concentrations of toluene and xylene isomers vs. axial distance for σ = 1,000, α = 1, ϕ = 100, f_o = 0.8, f_m = 0, f_p = 0.2.

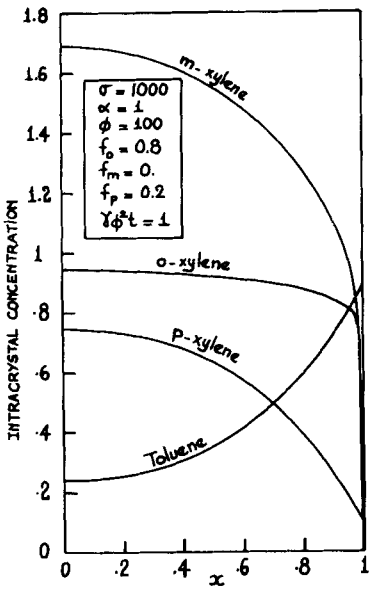

Figure 2a. Plots of intraparticle concentrations of toluene and xylene isomers at the axial location $\gamma\phi^2 t = 1$ for $\sigma = 1{,}000$, $\alpha = 1$, $\phi = 100$, $f_o = 0.8$, $f_m = 0$, $f_p = 0.2$.

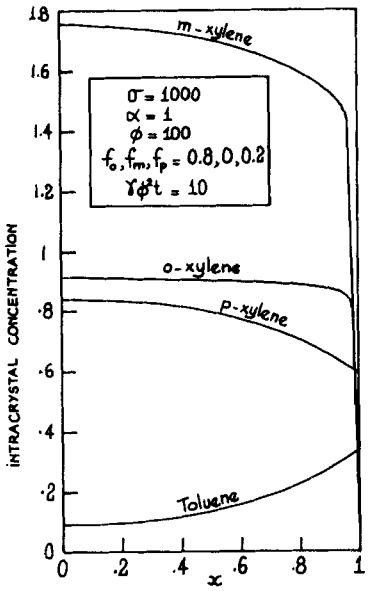

Figure 2b. Same as Figure 2 but at $\gamma\phi^2 t = 10$.

our theory is general and is applicable for any values of effective diffusivities and relative rate constants.

Figure 1 shows the concentrations of toluene and xylene isomers inside the reactor for $\sigma = 1{,}000$, $\alpha = 1$, $\phi = 100$, $f_o = 0.8$, $f_m = 0$, $f_p = 0.2$. For these values of parameters, the effective diffusivity of toluene is 1000 times greater than that of o-xylene ($\sigma = 1000$), the alkylation rate of toluene is the same order as the isomerization rate ($\alpha = 1$), the production of o- and m-xylene is *diffusion-controlled* ($\phi = 100$), and the primary distribution of xylene isomers contains mainly ortho and para-xylene, which is consistent with the fact that the substitution of the methyl group of toluene is para/ortho orientation. With this primary distribution (o, m, p = 0.8, 0, 0.2) the secondary distribution in the reactor contains mostly p-xylene (Figure 1). This is due to the steric hindrance imposed on the o- and m-xylene molecules. The m-xylene concentration in the reactor is seen to be higher than that of o-xylene. This is because the relative rate constants used in xylene isomerization are as follows:

$$o \underset{1}{\overset{2}{\rightleftharpoons}} m \underset{1}{\overset{2}{\rightleftharpoons}} p.$$

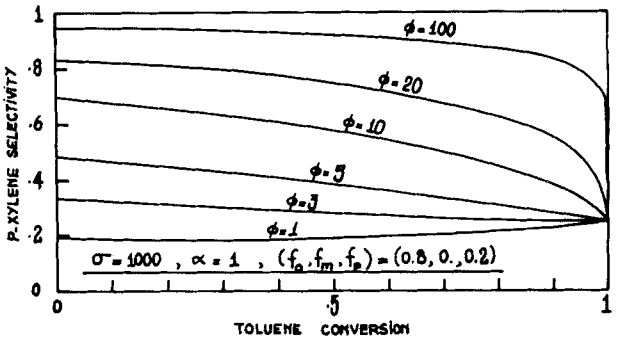

Figure 3. Plots of paraxylene selectivity vs. toluene conversion for various degrees of xylene isomerization for $\sigma = 1{,}000$, $\alpha = 1$, $f_o = 0.8$, $f_m = 0$, $f_p = 0.2$.

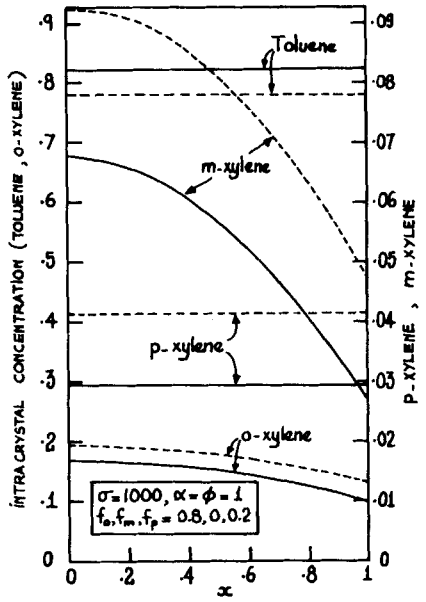

Figure 4. Plots of intraparticle concentrations of toluene and xylene isomers at the axial locations $\gamma\phi^2 t = 1$(—) and $\gamma\phi^2 t = 1.5$(---) for $\sigma = 1{,}000$, $\phi = 1$, $\alpha = 1$, $f_o = 0.8$, $f_m = 0$, $f_p = 0.2$.

For the same set of parameters used in Figure 1, the intracrystal concentrations of various species were plotted in Figures 2a and 2b at the reactor location $\gamma\phi^2 t = 1$ and 10, respectively. It is clear from Figure 2 that the intracrystal concentration profiles of m- and o-xylene are extremely sharp near the surface because of their steric restriction. The 1000 times faster in diffusion of p-xylene results in its rather shallow profile inside the crystal. It is the sharpness of o- and m-xylenes profiles that helps to increase the para selectivity in the reactor. The m-xylene intracrystal concentration is seen higher than o- and p-xylene concentrations in the inner core of the crystal because of the relative rate constants used in xylene isomerization.

Figure 3 shows the plot of paraxylene selectivity in xylene isomers [para/(para + ortho + meta)] vs. toluene conversion for various degrees of isomerization (i.e., for various ϕ). It is very interesting to note that for $\phi > \sim 3$, the para-xylene selectivity is better than the equilibrium selectivity of 25%. The paraxylene selectivity is greatly enhanced for large ϕ, that is, for large crystals and high temperatures. This is entirely consistent with the experimental findings of Young et al. (1982), Kaeding et al. (1981), and Chen et al. (1979). When ϕ is small, the selectivity at any level of toluene conversion (except 100%) is below the equilibrium selectivity. This is the case because at low values of ϕ, the diffusion effect does not play any role in the secondary distribution (i.e., the system is kinetic-controlled). This argument is further substantiated in Figure 4, where the intracrystal concentration profiles of all xylene isomers

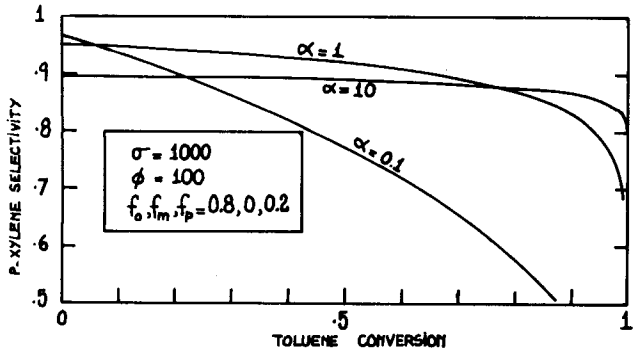

Figure 5. Plots of para-xylene selectivity vs. toluene conversion with α as parameter for σ = 1,000, ϕ = 100, f_o = 0.8, f_m = 0, f_p = 0.2.

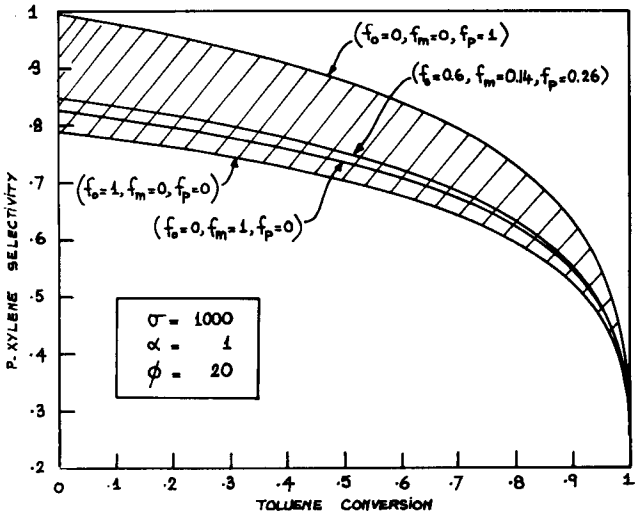

Figure 6. Plots of paraxylene selectivity vs. toluene conversion with the primary xylene distribution as parameter for σ = 1,000, α = 1, ϕ = 20.

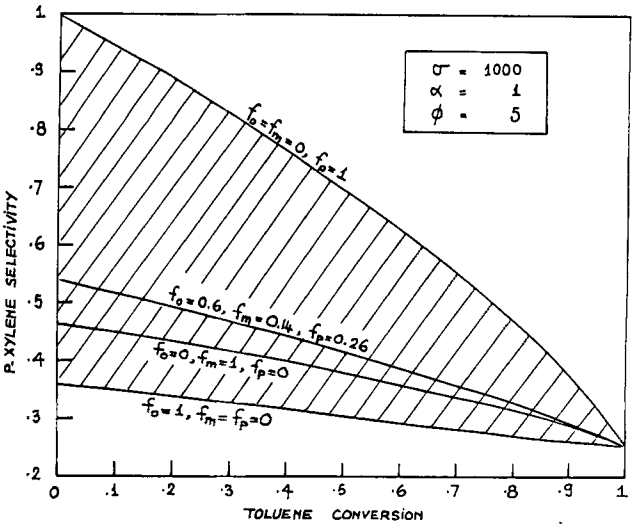

Figure 7. Plots of paraxylene selectivity vs. toluene conversion with the primary xylene distribution as parameter for σ = 1,000, α = 1, ϕ = 5.

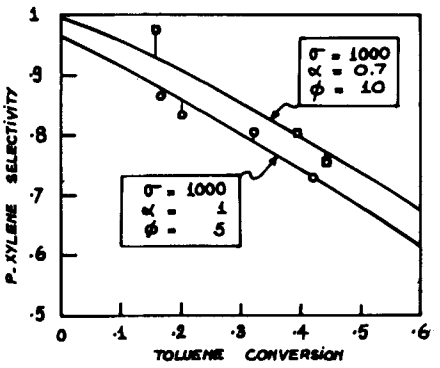

Figure 8. Comparison between theoretical prediction and the experimental data of Young et al. (13) for the alkylation of toluene with methanol using zeolite catalyst PZSM-5 (O: 550°C, □: 600°C).

are rather flat. Another reason why the paraxylene selectivity is lower than its equilibrium value is because the primary distribution is (o, m, p = 0.8, 0, 0.2). Had the primary distribution contained only p-xylene, the paraxylene selectivity would have been higher than the equilibrium value even for low values of ϕ.

It is noted that the paraxylene selectivity reaches the equilibrium value of 25% when the toluene conversion reaches 100% for all ϕ. This is entirely logical because if the reactor is sufficiently long, the p-xylene produced near the entrance of the reactor diffuses back into the particle as it proceeds along the reactor and isomerization is carried out; therefore, when toluene is eventually consumed, the equilibrium of isomerization prevails.

The effect of $\alpha = k_a/k_I$ on the paraxylene selectivity is shown in Figure 5. Increasing in α (that is, for paraselective zeolite catalyst; Young et al., 1982), the paraxylene selectivity is decreased slightly at very low toluene conversion, but this selectivity is maintained over a wide range of toluene conversion (see the curve for α = 10, Figure 5). For small α = 0.1 (that is, for nonselective zeolite catalyst), the paraxylene selectivity increases only slightly at extremely low toluene conversion but it then decreases sharply with increase in toluene conversion. In a way, nonselective zeolite catalyst is better at extremely low conversion, but this rather low conversion is impractical; therefore, the paraselective zeolite catalyst is preferable because the paraxylene selectivity is rather high and maintains so for a wide range of toluene conversion (up to 95% conversion).

The effect of primary distribution on the paraxylene selectivity versus toluene conversion is shown in Figures 6 and 7 for ϕ = 20 and 5, respectively. Two extremes of primary distribution (f_o = 1, $f_m = f_p = 0$ and $f_o = 0$, $f_m = 0$, $f_p = 1$) provide lower and upper bounds for paraxylene selectivity when other parameters are fixed. These bounds are close together when ϕ is very large (Figure 6), that is, the secondary distribution is independent of primary distribution when the catalyst is selective (i.e., for large ϕ). However, when ϕ is small (Figure 7), these two bounds are wide apart. That is, the secondary distribution of xylene isomers depends strongly on the primary distribution. The primary distribution of Friedel-Crafts reaction (f_o = 0.60, f_m = 0.14, f_p = 0.26; Allen and Yats, 1961) is also included in Figures 6 and 7. Obviously, the p-xylene selectivity calculated for this primary distribution lies betwen the two extremes described above.

The effect of toluene effective diffusivity was also studied, and insignificant change in the p-xylene selectivity was observed when the effective diffusivity of toluene was increased 10-fold.

Finally, to test our model solutions qualitatively, we attempted to fit our theoretical solutions with the Young et al. data for alkylation of toluene with methanol at 1 atm and T = 550 and 600°C. (See Figure 8.) At 550°C, we found that the theoretical solution with the following parameters, σ = 1,000, α = 1, ϕ = 5, f_o = .025, f_m = 0.025, f_p = 0.95, fits well with the experimental data. The theoretical solution with σ = 1,000, α = 0.7, ϕ = 10, $f_o = f_m = 0$, f_p = 1 fits well with the Young et al. data at T = 600°C. The theory predicts qualitatively with the experimental data (i.e., it shows the trend of the p-xylene selectivity versus toluene conversion) and the above parameters are one of the possible parameters to fit the experimental data because there is no information for diffusivities and relative rate constants for isomerization for the Young et al. system.

The theory presented so far is for the alkylation of toluene with methanol. However, the same procedure can be applied to solve

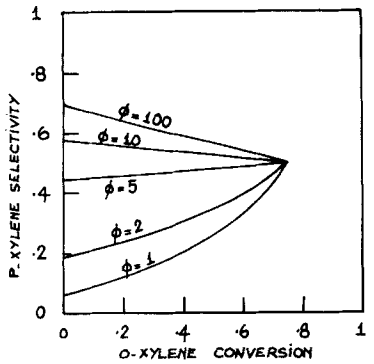

Figure 9. Plot of paraxylene selectivity vs. *o*-xylene conversion.

the case where the feed is pure *o*- or pure *m*-xylene. For this case, mass balance equations were derived and solved. When *o*-xylene is the only reactant, the selectivity of *p*-xylene to *m*-xylene vs. *o*-xylene conversion is plotted in Figure 9. For this case, the equilibrium selectivity is 50%. Similarly, as in the case of the alkylation of toluene with methanol, the selectivity is greater than the equilibrium value of 50% when ϕ is large, and the reverse is true when ϕ is small.

ACKNOWLEDGMENT

This work was partially supported by a special Project Grant of the University of Queensland. The author wishes to thank one of the referees for pointing out the chemistry aspect of this system.

NOTATION

a = defined in Eq. 27a
$\boldsymbol{A}$ = matrix, defined in Eq. 22
b = defined in Eq. 27b
c = defined in Eq. 27c
C = concentration
$\boldsymbol{C}$ = matrix, defined in Eq. 36
d = defined in Eq. 27d
$\mathcal{D}_T$ = effective diffusivity of toluene
$\mathcal{D}_o$ = effective diffusivity of *o*- and *m*-xylene
$\boldsymbol{D}$ = matrix, defined in Eq. 31
e = defined in Eq. 27e
f_m = primary distribution of *m*-xylene
f_o = primary distribution of *o*-xylene
f_p = primary distribution of *p*-xylene
k_a = rate constant for alkylation reaction
k_I = rate constant for isomerization
K_n = transform kernel, defined in Eq. 17
$\boldsymbol{K}$ = matrix, defined in Eq. 23
r = radial coordinate
R = crystal radius
S = selectivity of *p*-xylene
t = nondimensional axial coordinate
$\bar{u}$ = superficial velocity
y_j = nondimensional intracrystal concentration of species j
u_{bj} = nondimensional reactor concentration of species j
$\boldsymbol{U}_b$ = vector, defined in Eq. 21
v_j = defined in Eq. 12
$\boldsymbol{V}$ = vector, defined in Eq. 29
x = nondimensional radial coordinate
X = toluene conversion
z = axial coordinate

Greek Letters

α = parameter, defined in Eq. 6
β_{ij} = defined in Eq. 26
γ = parameter, defined in Eq. 6
ϵ_b = reactor voidage
ϕ = Thiele modulus, defined in Eq. 6
σ = parameter, defined in Eq. 6
ξ_n = eigenvalue, defined in Eq. 18
$\boldsymbol{\Omega}$ = vector, defined in Eq. 20

Subscripts

1 = *t*oluene
2 = *o*-xylene
3 = *m*-xylene
4 = *p*-xylene
b = bulk concentration
$\langle,\rangle$ = integral transform, defined in Eq. 16

LITERATURE CITED

Allen, R. H., and L. D. Yats, "Kinetics of Three-Compound Equilibrations. V. Concurrent Alkylation and Isomerization," *J. Amer. Chem. Soc.*, **83**, 2799 (1961).

Chen, N. Y., W. W. Kaeding, and F. G. Wyer, "Para-Directed Aromatic Reactions over Shape Selective Molecular Sieve Zeolite Catalysts," *J. Amer. Chem. Soc.*, **101**, 6783 (1979).

Chutoransky, P., and F. G. Dwyer, "Effect of Zeolite Crystallite Size on the Selectivity Kinetics of the Heterogeneous Catalyzed Isomerization of Xylenes," *Adv. Chem. Ser.*, **121**, 540 (1973).

Collins, D. J., K. J. Mulrooney, R. J. Medina, and B. H. Davis, "Xylene Isomerization and Disproportionation over Lanthanum Y Catalyst," *J. Catal.* **75**, 291 (1982).

Cortes, A., and A. Corma, "The Mechanism of Catalytic Isomerization of Xylenes: Kinetics and Isotopic Studies," *J. Catal.*, **51**, 338 (1978).

Hanson, K. L., and A. J. Engel, "Kinetics of Xylene Isomerization over Silica-Alumina Catalyst," *AIChE J.*, **13**, 260 (1967).

Kaeding, W. W., C. Chu, L. B. Young, B. Weinstein, and S. A. Butter, "Selective Alkylation of Toluene with Methanol to Produce Para-Xylene," *J. Catal.*, **67**, 159 (1981).

Röbschläger, K. H., and E. G. Christoffel, "Kinetic Investigation of the Isomerization of C_8-Aromatics," *Can. J. Chem. Eng.*, **58**, 517 (1980).

Silvestri, A. J., and C. D. Prater, "Kinetic Studies of the Selectivity of Xylene Isomerization over Silica-Alumina Catalyst," *J. Phys. Chem.*, **68**, 3268 (1964).

Sneddon, I. N., *The Use of Integral Transform*, McGraw-Hill, New York (1972).

Venuto, P. B., L. A. Hamilton, and P. S. Landis, "Organic Reactions Catalyzed by Crystalline Aluminosilicates. II. Alkylation Reactions: Mechanistic and Aging Considerations," *J. Catal.*, **5**, 484 (1966).

Wei, J., "Intraparticle Diffusion Effects in Complex Systems of First-Order Reactions. I. The Effects in Single Particles," *J. Catal.*, **1**, 526 (1962a).

——, "Intraparticle Diffusion Effects in Complex Systems of First Order Reactions. II. The Influence of Diffusion on the Performance of Chemical Reactors," *J. Catal.*, **1**, 538 (1962b).

——, "A Mathematical Theory of Enhanced Para-Xylene Selectivity in Molecular Sieve Catalysts," *J. Catal.*, **76**, 433 (1982).

Weisz, P. B., and V. J. Frilette, "Intracrystalline and Molecular-Shape-Selective Catalysis by Zeolite Salts," *J. Phys. Chem.*, **64**, 382 (1960).

Yashima, T., H. Ahmad, K. Yamazaki, M. Katsuta, and N. Hara, "Alkylation on Synthetic Zeolites. I. Alkylation of Toluene with Methanol," *J. Catal.*, **16**, 273 (1970a).

Yashima, T., K. Yamazaki, H. Ahmad, M. Katsuta, and N. Hara, "Alkylation on Synthetic Zeolites. II. Selectivity of *p*-Xylene Formation," *J. Catal.*, **17**, 151 (1970b).

Yashima, T., K. Sato, T. Hayasaka, and N. Hara, "Alkylation on Synthetic Zeolites," II. Alkylation of Toluene with Methanol and Formaldehyde on Alkali Cation Exchanged Zeolites," *J. Catal.*, **26**, 303 (1972).

Young, L. B., S. A. Butter, and W. W. Kaeding, "Shape Selective Reactions with Zeolite Catalysts. III. Selectivity in Xylene Isomerization, Toluene-Methanol Alkylation, and Toluene Fisproportionation over ZSM-5 Zeolite Catalysts," *J. Catal.*, **76**, 418 (1982).

Manuscript received May 17, 1983; revision received June 5, 1984, and accepted June 8.